ISSN 0036-0236, Russian Journal of Inorganic Chemistry, 2015, Vol. 60, No. 5, pp. 595–601. © Pleiades Publishing, Ltd., 2015.
Original Russian Text © O.V. Konnik, V.F. Shul'gin, E.A. Zamnius, A.N. Gusev, V.V. Minin, 2015, published in Zhurnal Neorganicheskoi Khimii, 2015, Vol. 60, No. 5, pp. 664–671.

PHYSICAL METHODS OF INVESTIGATION

Trinuclear Copper(II) Complexes Based on Iminodiacetic Acid Salicylidenehydrazone

O. V. Konnik, V. F. Shul'gin, E. A. Zamnius, A. N. Gusev, and V. V. Minin

Kurnakov Institute of General and Inorganic Chemistry, Russian Academy of Sciences, Leninskii pr. 31, Moscow, 117907 Russia

e-mail: vshul@crimea.edu

Received November 11, 2014

Abstract—Nickel, copper, and zinc complexes with salicylidenehydrazone of iminodiacetic acid (H_4L): $Cu_2L \cdot 2Py \cdot 2CH_3OH$ and $Cu_2ML(CH_3COO)_2$ (M= Ni, Cu, Zn) were synthesized and studied by thermogravimetric analysis and IR and ESR spectroscopy. The crystal structure of the complex $Cu_2ZnL(CH_3COO)_2 \cdot 4Py \cdot CH_3OH$ was studied by X-ray diffraction: space group $C2/c$, $a = 31.6974(12)$ Å, $b = 10.3023(4)$ Å, $c = 16.4714(7)$ Å; $\beta = 119.7460(10)°$; $Z = 4$; 3513 reflections with $I > 2\sigma(I)$; $R = 0.0382$, $R_w = 0.1010$. The temperature dependences of the ESR spectra of liquid solutions and the magnetic susceptibility of polycrystalline samples were studied. The ESR spectra of the binuclear copper complex and the trinuclear dicopper zinc complex exhibited hyperfine structure of seven lines, indicating exchange interaction of unpaired electrons with two equivalent copper nuclei.

DOI: 10.1134/S0036023615050125

Polynuclear coordination compounds of metals with nitrogen-containing organic ligands arouse enhanced interest as structural and functional models of metalloproteins [1, 2]. The interest in trinuclear copper(II) complexes is related, first of all, to studies of mechanisms of some biochemical reactions [3–6]. The exchange-coupled polynuclear copper(II) complexes can also serve as the base for the design of porous magnetic materials [7].

According to published data, salicylidenehydrazones of pyridinedicarboxylic and iminodiacetic acids are convenient ligands for the design of trinuclear copper(II) complexes [8–10]. Usually these complexes form oligomeric or polymeric structures. The molecular trinuclear complexes obtained from these ligands are only few in number [9]. This communication describes the binuclear copper(II) complex with bis(salicylidenehydrazone) of iminodiacetic acid (H_4L) and heteronuclear complexes based on this ligand.

EXPERIMENTAL

Synthesis of $Cu_2L \cdot 2Py \cdot 2CH_3OH$ (I). Salicylaldehyde (1.35 g, 11 mmol) was added to a suspension of iminodiacetic acid hydrazide (0.81 g, 5 mmol) in methanol (30 mL). The reaction mixture was magnetically stirred at reflux for 2 h. The precipitate was allowed to stand for 12 h. Copper(II) acetate monohydrate (2.0 g, 10 mmol) was added to the resulting suspension and the mixture was stirred at reflux. After 12 h, a dark green precipitate formed, which was filtered off and dried in air. The compound thus obtained was dissolved in a minimum amount of pyridine, and water (200 mL) was added. After 24 h, the precipitate that formed was filtered off, washed with a small amount of ethanol and water, and dried in air to a constant weight. The yield of the complex was 85% of the theoretically possible yield.

$Cu_2L \cdot 2Py \cdot 2CH_3OH$ (**I**).

For $C_{30}H_{23}N_7O_6Cu_2$ ($M = 704.65$) anal. calcd. (%): C, 51.18; H, 3.27; N, 13.93.

Found (%): C, 50.55; H, 4.16; N, 13.59.

IR (KBr), ν, cm^{-1}: 1616, 1601, 1532, 1443, 1416, 1292, 1199, 1152, 906, 754.

Synthesis of $Cu_2NiL(CH_3COO)_2 \cdot 4Py \cdot CH_3OH$ (II). Pyridine was added dropwise to a suspension of complex **I** (1.1 g, 2 mmol) in ethanol (30 mL) until the solid dissolved. An equivalent amount of nickel acetate (2 mmol) was added to the resulting solution and the mixture was stirred with heating for 1 h. The solution was filtered and allowed to stand for 24 h. The dark green precipitate that formed was filtered off, washed with a small amount of ethanol, and dried in air to a constant weight. The yield of the complex was 60% of the theoretically possible yield.

$Cu_2NiL(CH_3COO)_2 \cdot 4Py \cdot CH_3OH$ (**II**).

For $C_{43}H_{44}N_9O_9Cu_2Ni$ ($M = 1016.66$) anal. calcd. (%): C, 51.01; H, 4.68; N, 12,51.

Found (%): C, 50.74; H, 4.33; N, 12.39.

IR (KBr), ν, cm^{-1}: 1539, 1443, 1384, 1335, 1303, 1197, 1149, 906, 754, 698.

The synthesis of $Cu_2ZnL(CH_3COO)_2 \cdot 4Py \cdot CH_3OH$ (III) was carried out using zinc acetate by the same procedure as compound **II**. The product yield was 60%.

$Cu_2ZnL(CH_3COO)_2 \cdot 4Py \cdot CH_3OH$ (**III**).

For $C_{43}H_{44}N_9O_9Cu_2Zn$ (M = 1023.36) anal. calcd. (%): C, 51.01; H, 4.68; N, 12.31.

Found (%): C, 50.62; H, 4.22; N, 12.45.

IR (KBr), ν, cm^{-1}: 1620, 1544, 1448, 1378, 1298, 1198, 1152, 1074, 904, 755, 698.

The synthesis of $Cu_3L \cdot 4Py \cdot CH_3OH$ (IV) was carried out by the same procedure using copper acetate. The product yield was 65%.

$Cu_3L \cdot 4Py \cdot CH_3OH$ (**IV**).

For $C_{43}H_{44}N_9O_9Cu_3$ (M = 1021.52) anal. calcd. (%): C, 50.37; H, 4.95; N, 12.17.

Found (%): C, 49.41; H, 4.31; N, 12.34.

IR (KBr), ν, cm^{-1}: 1618, 1598, 1545, 1445, 1380, 1305, 1202, 756, 700.

The IR spectra of samples pressed with KBr were studied in the 4000–400 cm^{-1} range on a Perkin Elmer Spectrum BX FT IR spectrometer.

The elemental analysis for carbon, hydrogen, and nitrogen was performed on a Perkin-Elmer 240C analyzer by burning the sample in an oxygen flow and subsequent chromatography of the gaseous products in a helium flow.

The thermograms were measured on a Paulik-Paulik-Erdey Q-derivatograph in a static air atmosphere, at a heating rate of 10 K/min, using a ceramic crucible without a lid as the sample holder and calcined alumina as the reference.

The ESR spectra of liquid solutions ($C \sim 3 \times 10^{-3}$ mol/L) were recorded on an ADANI PS 100.X spectrometer in the X-range. A toluene–pyridine mixture (1 : 1 v/v) was used as the solvent and DPPH served as the reference.

The spectra were theoretically simulated with a program package described in a monograph [11]. The sum of Lorentzian and Gaussian functions was used as the line shape function. According to the relaxation theory, one-center contributions to the line width were specified by the expression

$$\Delta H_p = \alpha + \beta m_I + \gamma m_I^2, \quad (1)$$

where m_I is the nuclear spin projection; α, β, and γ are line width parameters. The term α takes into account broadening effects that are the same for all HFS lines. The β factor is defined as the product of the g-tensor by the hyperfine coupling tensor. The γ factor is related to the HFS anisotropy and depends on the correlation time of the paramagnetic species rotational motion in the liquid.

The simulation also takes into account the contribution caused by the intramolecular motion in the binuclear complex

$$\Delta H_p(1,2) = \delta(m_{I1} - m_{I2})^2. \quad (2)$$

The parameters g_0, a_{Cu}, α, β, γ, and δ were varied to reach a minimum of the error functional.

$$F = \frac{1}{N}\left[\sum_{i=1}^{N}\left(Y_i^E - Y_i^T\right)^2\right]. \quad (3)$$

The temperature varioations of the magnetic susceptibility were measured on a SQUID magnetometer (MPMS-XL7, Quantum Design) in the temperature range of 2–300 K at an external magnetic field strength of 5000 Oe. The experimental data were corrected with allowance for the diamagnetic contribution of the ligands using the Pascal additive scheme [12].

The X-ray diffraction analysis of a single crystal of **III** grown from a methanol–pyridine mixture was performed at 296 K on a Bruker Smart APEX II diffractometer equipped by a CCD detector (MoK_α, graphite monochromator) using a standard procedure [13]. The absorption corrections were applied by the azimuthal scanning method. The structure was solved by the direct method and refined by least squares in the full-matrix anisotropic approximation using SHELXS-97 and SHELXL-97 software [14]. The hydrogen atoms were generated geometrically and refined in the "riding" model. The X-ray experiment and structure solution and refinement details are summarized in the table. The full set of data is deposited with the Cambridge Crystallographic Data Centre (No. CCDC 1025187 deposit@ccdc.cam.ac.uk or http://www.ccdc.cam.ac.uk/data_request/cif).

RESULTS AND DISCUSSION

Previously it was shown that the reaction of salicylidenehydrazone of iminodiacetic acid with copper(II) perchlorate or nitrate in 1 : 3 ratio and subsequent recrystallization of the reaction product from dimethyl sulfoxide gives a coordination polymer in which trinuclear complexes are linked into a chain via phenoxide bridges [10]. According to our study, the reaction of iminodiacetic acid salicylidenehydrazone with copper(II) acetate in 1 : 2 ratio followed by treatment of the product with pyridine yields the binuclear complex in which the monomeric subunits are linked by the iminodimethylene bridge. Owing to the presence of free donor sites, this complex can be used as a synthon in the preparation of trinuclear coordination compounds. For instance, reactions of complex **I** with nickel, copper, or zinc acetate gave trinuclear complexes containing a heterometallic copper···nickel (copper, zinc)···copper chain.

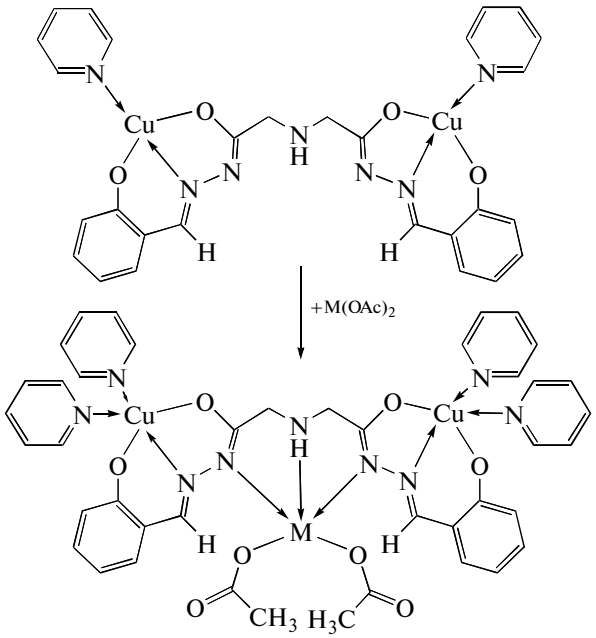

The composition of complexes was confirmed by elemental analysis data. Unfortunately, the thermograms of most compounds proved to be of little use due to overlap of desolvation and oxidative destruction of the organic ligand. In the thermogram of complex **I**, these processes are recorded separately. In the 60–200°C temperature range, a 9% mass loss takes place accompanied by a small endotherm with a minimum in the DTA curve at 110°C corresponding to the removal of two methanol molecules. In the 200–250°C temperature range, the mass loss is 11%, the minimum in the DTA curve being at 230°C, which corresponds to the loss of one pyridine molecule. Immediately after completion of this process, thermooxidative destruction of the complex starts and then smoothly transforms into burning-out of the organic residue, which is accompanied by a broad exotherm; the maximum in the DTS curve is at 400°C. The process is completed at 650°C at 73% mass loss of the sample.

The IR spectra of complexes **I**–**IV** no longer exhibit the amide-1 band observed in the spectra of free salicylidenehydrazone at 1661 cm^{-1} but exhibit a new absorption band with a peak at 1532–1544 cm^{-1}, which was assigned to the stretching vibrations of the azomethine bond system >C=N–N=C<. Attention is drawn by the disappearance of the bands with peaks at 3190 and 3050 cm^{-1}, corresponding to NH and OH vibrations of salicylidenehydrazone, indicating that the ligand has been protonated upon coordination.

The asymmetric stretching mode of the carboxyl group in the IR spectrum of complex **IV** occurs at 1620 cm^{-1}, which is typical of coordinated monodentate carboxylate ligands. For complexes **II** and **III**, the $\nu_{as}(COO^-)$ mode is shifted to lower frequency and is superimposed onto the azomethine stretching band. This may be caused by both the bidentate coordination of the acetate anion and the formation of strong hydrogen bonds, which mitigates the difference between the asymmetric and symmetric stretching frequencies. Previously, a similar phenomenon was described for zinc 2-methyl-4-chlorophenoxyacetate in which the formation of strong hydrogen bonds reduces the $\Delta\nu(COO^-)$ of the monodentate carboxyl group to a value typical of coordinated bidentate carboxylate anions (170 cm^{-1}) [15, 16].

X-ray experiment details and structure solution and refinement data for complex **III**

Parameter	Value
Molecular formula	$C_{42}H_{45}Cu_2N_9O_{12}Zn$
Crystal size, mm	0.45 × 0.50 × 0.30
FW	1060.32
System	Monoclinic
Space group	*C*2/*c*
a, Å	31.6974(12)
b, Å	10.3023(4)
c, Å	16.4714(7)
β, deg	119.7460(10)
Z	4
V, Å^3	4670.1(3)
T, K	296(2)
μ, mm^{-1}	1.482
ρ_{calcd}, g cm^{-3}	1.543
Range of θ, deg	2.11–26.50
Range of indices	$-39 < h < 30$
	$-12 < k < 10$
	$-20 < l < 20$
The number of measured reflections	22499
The number of independent reflections	4832
The number of reflections with $I > 2\sigma(I)$	3513
The number of refined parameters	319
R*	0.0382
R_w^*	0.1010
GOOF	1.060
$\Delta\rho_{max}$, $\Delta\rho_{min}$, e Å^{-3}	0.723, –0.523

The unambiguous structure determination for the complexes was based on single crystal X-ray diffraction of **III**. The general view of the molecule and the lengths of bonds involving metal cations are summarized in Fig. 1.

The complex has a molecular structure with usual bond lengths and bond angles [17, 18]. The coordination polyhedron of the copper cation can be described

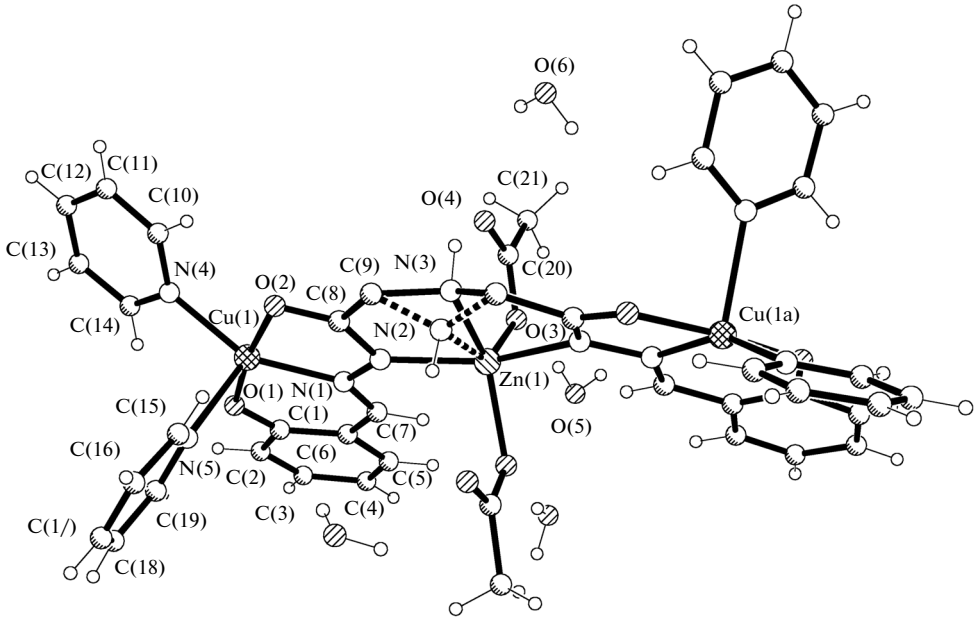

Fig. 1. Molecular structure of $Cu_2ZnL(CH_3COO)_2 \cdot 2Py \cdot 4H_2O$ (**III**). Lengths of bonds involving metal cations: Zn(1)–O(3), 2.0388(19); Zn(1)–N(2), 2.076(2); Zn(1)–N(3), 2.139(5); Zn(1)–O (3), 2.0388(19); Zn(1)–N(2), 2.076(2); Zn(1)–N(3), 2.139(5); Cu(1)–O(1), 1.903(2); Cu(1)–O(2), 1.9900(19); Cu(1)–N(5), 2.279(3); Cu(1)–N(1), 1.940(2); Cu(1)–N(4), 2.042(2) Å.

as a distorted tetragonal pyramid with the Addison parameter $\tau = 0.34$ [19]. The copper atom deviates from the pyramid base by 0.264 Å toward the nitrogen atom that forms the vertex. The chelate rings are somewhat arched and non-coplanar, the angle between them being 6.1°.

The coordination polyhedron of the zinc cation is a highly distorted trigonal bipyramid with the N(2) and N(2)' atoms at the vertices ($\tau = 0.86$). The imine nitrogen atom N(3) and the hydrogen atom it bears are disordered over two positions around a twofold axis. The acetate anions are bonded to zinc in the monodentate fashion; the oxygen–carbon bond lengths differ considerably from one another. Water molecules are located in the outer sphere and are bonded by strong hydrogen bonds to one another and to the oxygen atoms of the coordinated acetate anions.

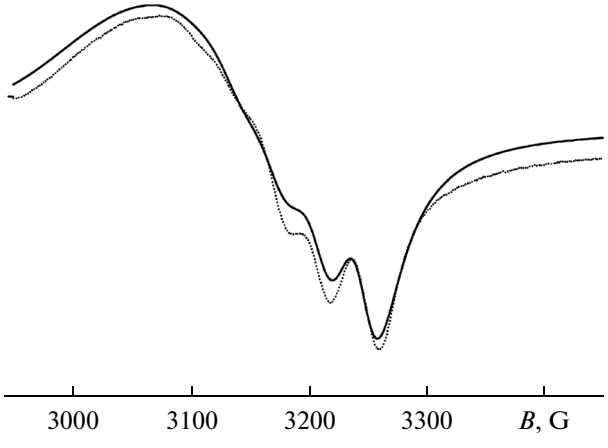

Fig. 2. ESR spectrum of complex **I** at 293 K (pyridine–toluene). The continuous line is the experimental spectrum, the dotted line is the simulated spectrum.

According to powder X-ray diffraction data, complexes **II** and **IV** are isostructural to the copper–zinc analog.

The binuclear structure of complex **I** is confirmed by the ESR spectrum. At room temperature, the spectrum shows poorly resolved hyperfine structure due to the two equivalent copper nuclei (Fig. 2). An increase in the solution temperature to 353 K improves the spectrum quality; in this case, the HFS consisting of seven lines with intensity ratio of 1 : 2 : 3 : 4 : 3 : 2 : 1 can be clearly seen, which is indicative of exchange interaction of unpaired electrons with two equivalent copper nuclei (Fig. 3). The spin Hamiltonian parameters remain almost invariable ($g_0 = 2.117$ and $a_{Cu} = 36.6 \times 10^{-4}$ cm^{-1}), while line width parameters α, β, and γ regularly decrease and δ increases from 0.002 to 1.38.

The ESR spectrum of the solution of the copper zinc complex **III** at room temperature exhibits a poorly resolved signal of seven HFS lines with effective

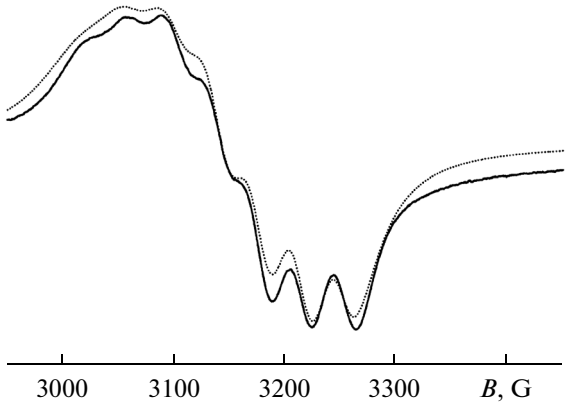

Fig. 3. ESR spectrum of complex **I** at 353 K (pyridine–toluene). The continuous line is the experimental spectrum, the dotted line is the simulated spectrum.

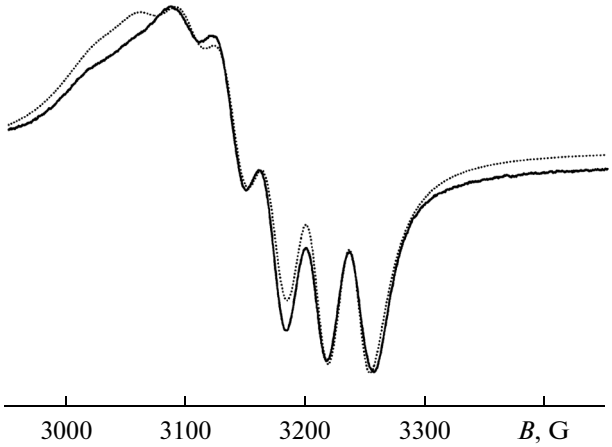

Fig. 4. ESR spectrum of a solution of **III** at 353 K (pyridine–toluene). The continuous line is the experimental spectrum, the dotted line is the simulated spectrum.

spin Hamiltonian parameters close to those of the initial spacered copper complex. A temperature rise to 353 K enhances the spectral resolution, and the seven HFS lines are clearly seen (Fig. 4). The *g*-factors and the HFS constants of complexes **I** and **III** ($g_0 = 2.118$ and $a_{Cu} = 34.1 \times 10^{-4}$ cm^{-1}) differ insignificantly, which indicates either elimination of the zinc cation in solution or weak effect of the diamagnetic cation on the exchange channels if the trinuclear structure is retained. The complexes differ noticeably in the line width parameters, which attests for the retention of the trinuclear structure. This is especially true for the parameter δ related to the intramolecular motion of the copper coordination polyhedra relative to each other; in complex **III** this parameter is zero. Evidently, the zinc cation coordinates the donor nitrogen atoms of two mononuclear subunits, thus preventing them from moving relative to each other.

The spectrum of a solution of complex **III** frozen at 77 K is typical of axially symmetric systems ($g_\parallel = 2.04$; $g_\perp = 2.30$). In the parallel orientation region, the HFS due to two equivalent copper nuclei can be clearly seen ($A_\parallel = 120$ G) (Fig. 5).

In the earlier studies of spacered binuclear copper(II) complexes by the static magnetic susceptibility technique, weak intramolecular exchange interactions comparable in energy with intermolecular interactions, were detected [20, 21]. Magnetochemical investigation of complexes **I** and **III** lead to a similar result.

The temperature dependence curve of magnetic susceptibility for complex **I** is shown in Fig. 6. As can be seen from the Figure, a decrease in temperature induces smooth and then fast increase in the magnetic susceptibility to reach a maximum at 6 K. Further lowering of the temperature results in a decrease in χ. The effective magnetic moment of the complex at 300 K is 2.65 μB and is close to 2.45 μB, which is a value expected for two non-interacting copper(II) cations. Lowering the temperature to 4 K results in a decrease in the effective magnetic moment to 0.66 μB (Fig. 6), indicating the occurrence of antiferromagnetic interactions between the paramagnetic centers. The experimental data are well approximated by the modified Bleany–Bowers equation [22]

$$\chi = 2\frac{N_A\mu_B^2 g^2}{kT}\frac{1}{3+\exp(-2J/kT)} \times (1-p) + \frac{N_A g^2 \mu_B^2}{4kT}p + N\alpha, \quad (4)$$

where $-2J$, p, and N_α are the singlet–triplet splitting energy, the paramagnetic monomer impurity, and the temperature-independent paramagnetism. The other designations are usual.

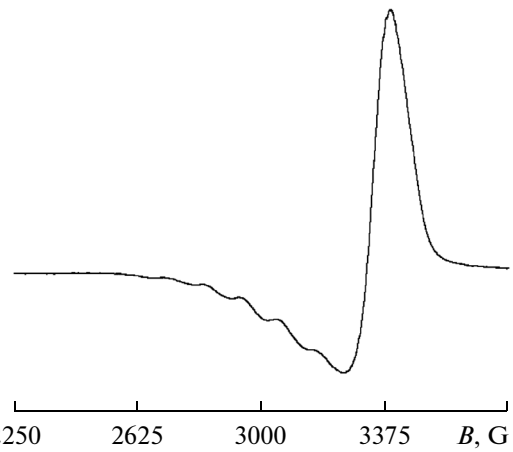

Fig. 5. ESR spectrum of a frozen solution of **III** at 77 K (pyridine–toluene).

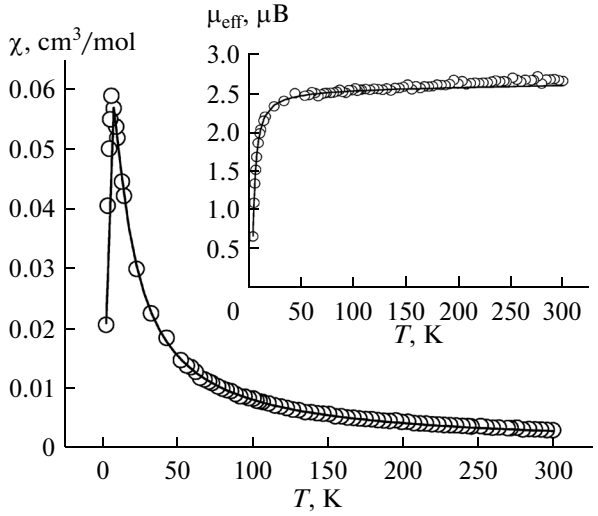

Fig. 6. χ and μ_{eff} vs. temperature for **I** (The continuous line is the theoretical curve).

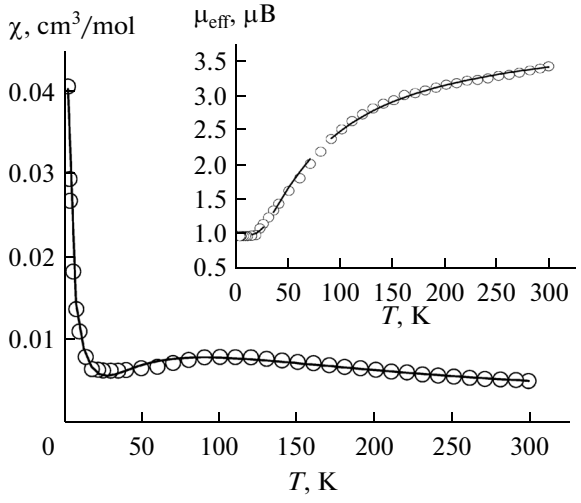

Fig. 7. χ and μ_{eff} vs. temperature for **II** (The continuous line is the theoretical curve).

The exchange interaction parameters determined upon the simulation are close to the values observed previously for other spacered binuclear copper(II) complexes ($-2J = 6.6$ cm^{-1} and $g = 2.095$; $R = \Sigma(\chi_{theor} - \chi_{exp})^2/\Sigma(\chi_{exp})^2 = 2.2 \times 10^{-4}$).

Study of the temperature dependence of the magnetic susceptibility for complex **III** also attests to weak exchange interactions. The simulation of the temperature dependence of the magnetic susceptibility by the Bleany–Bowers equation in terms of the isolated dimer model gives the following values of the variable parameters: $g = 2.089$ and $-2J = 3.75$ cm^{-1}; $R = 2.5 \times 10^{-5}$.

To elucidate the effect of the nature of the central atom on the magnetic properties of heteronuclear complexes, temperature variations of the magnetic susceptibility for **II** and **IV** were studied. The magnetic moment of the heteronuclear complex **II** at room temperature is 3.41 μB, i.e., it is lower than the value expected for a non-interacting system Cu(II)–Ni(II)–Cu(II) (4.11 μB). As the temperature is lowered, the effective magnetic moment decreases to reach a constant value of $\mu_{eff} \approx 1$ at 21 K. The temperature dependence of the magnetic susceptibility shows that the nickel ion with $S = 1$ is antiferromagnetically coupled with the terminal copper(II) ions with $S = 1/2$. As the temperature decreases, χ slightly increases to reach a maximum at 100 K, then decreases to 30 K, and sharply increases below 17 K (Fig. 7).

The use of spin Hamiltonian (5), which takes into account the interaction of the nickel cation with two copper cations and neglects the interaction of the copper cations with each other, makes it possible to derive equation (6), describing the temperature dependence of magnetic susceptibility for complex **II**.

$$H = -2J(S_{Cu1}S_{Ni} + S_{Cu2}S_{Ni}), \quad (5)$$

$$\chi = \frac{2N\beta^2g^2}{kT}\left(\frac{1 + 5e^{4J/kT} + e^{2J/kT}}{3 + 5e^{4J/kT} + e^{-2J/kT} + 3e^{2J/kT}}\right). \quad (6)$$

The correction for the paramagnetism of the monomeric impurity with the mole fraction p was performed using equation (7) [23].

$$\chi'_M = \chi_M(1 - p) + \frac{N\beta^2g^2}{3kT} \times 3.5p + N_\alpha, \quad (7)$$

$$N_\alpha = 400 \times 10^{-6} \text{ cm}^3/\text{mol}.$$

The theoretical simulation of the temperature dependence of the magnetic susceptibility gives the following values of variable parameters: $g = 1.91$ and $-2J = 42$ cm^{-1}; $R = 5.7 \times 10^{-4}$.

The temperature dependence of the magnetic susceptibility and the effective magnetic moment for trinuclear complex **IV** is presented in Fig. 8. At room temperature, the effective magnetic moment is 2.54 μB, which is much lower than the value expected for three non-interacting copper ions (3.23 μB for $g = 2.15$ characteristic of this type of complexes).

The decrease in the magnetic moment with temperature decrease indicates the occurrence of rather strong exchange interaction between the paramagnetic centers. Below 70 K, the magnetic moment almost does not decrease, being 1.83 μB, which implies the ground state with $S = 1/2$. If the interaction between the terminal copper atoms is neglected, the spin Hamiltonian for the Cu–Cu–Cu system has the form [24]:

$$H = -2J(S_{Cu1}S_{Cu2} + S_{Cu1}S_{Cu2}). \quad (8)$$

The expression for the temperature dependence of the magnetic susceptibility derived using Hamiltonian (8) has the form

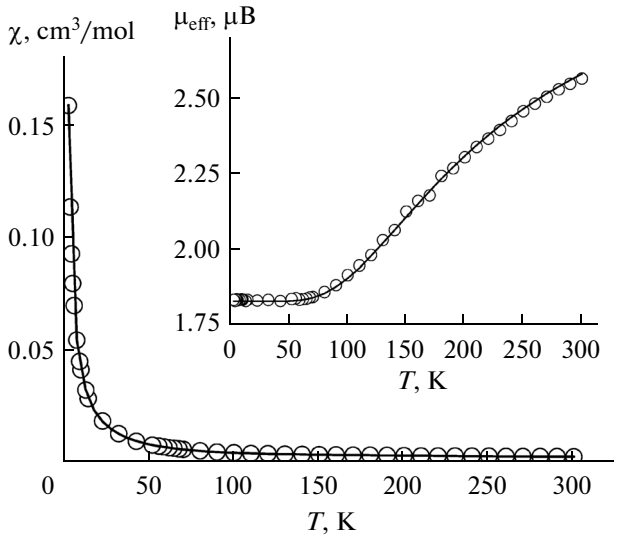

Fig. 8. χ and μ_{eff} vs. temperature for **IV** (The continuous line is the theoretical curve).

$$\chi = \frac{N\beta^2 g^2}{4kT}\left(\frac{1+e^{-J/kT}+10e^{-3J/kT}}{1+e^{J/kT}+2e^{-3J/kT}}\right). \quad (9)$$

The simulation of the temperature dependence of the magnetic susceptibility within the framework of this model gives $g = 2.111$ and $-J = 207\ \text{cm}^{-1}$; $R = 1.4 \times 10^{-5}$.

Thus, the results of the study indicate that the use of bis(salicylidenehydrazone) of iminodiacetic acid as the proligand allows the synthesis in good yields of linear homo- and heterometallic coordination compounds distinguished by intense antiferromagnetic exchange interactions of the paramagnetic cation that occupies the central position with the terminal ions.

ACKNOWLEDGMENTS

This work was supported by the Russian Foundation for Basic Research, project no. 13-03-00703.

REFERENCES

1. W. Luo, X.-G. Meng, J.-F. Xiang, et al., Inorg. Chim. Acta **361**, 2667 (2008).
2. O. Das, E. Zangrando, and T. K. Paine, Inorg. Chim. Acta **362**, 3617 (2009).
3. E. I. Solomon, U. M. Sundaram, and T. E. Machonkin, Chem. Rev. **96**, 2563 (1996).
4. L. M. Mirica and T. D. P. Stack, Inorg. Chem. **44**, 2131 (2005).
5. J. Yoon and E. I. Solomon, Coord. Chem. Rev. **251**, 379 (2007).
6. H. Borzel, P. Comba, and H. Pritzkow, Chem. Commun., No. 1, 97 (2001).
7. S. S.-Y. Chui, S. M.-F. Lo, J. P. H. Charmant, et al., Science **283** (5405), 1148 (1999).
8. X. Chen, S. Zhan, C. Hu, et al., J. Chem. Soc., Dalton Trans., No. 2, 245 (1997).
9. V. A. Milway, L. Zhao, T. S. M. Abedin, et al., Polyhedron **22**, 1271 (2003).
10. H. Adams, D. E. Fenton, and G. Minardi, Inorg. Chem. Commun. **3**, 24 (2000).
11. Yu. V. Rakitin, G. M. Larin, and V. V. Minin, *Interpretation of EPR Spectra of Coordination Compounds* (Nauka, Moscow, 1993) [in Russian].
12. Yu. V. Rakitin and V. T. Kalinnikov, *Advanced Magnetochemistry* (Nauka, St. Petersburg, 1994) [in Russian]
13. SMART (Control) and SAINT (Integration) Software, Version 5.0, Bruker AXS, Inc., Madison (WI), 1997.
14. G. M. Sheldrick, Acta Crystallogr., Sect. A **64**, 112 (2008).
15. S. E. Nefedov, Yu. T. Struchkov, O. V. Konnik, et al., Ukr. Khim. Zh. **57**, 685 (1991).
16. O. V. Konnik, V. F. Shul'gin, S. E. Nefedov, et al., Zh. Neorg. Khim. **36**, 630 (1991).
17. G. Orpen, L. Brammer, F. H. Allen, et al., J. Chem. Soc., Dalton Trans. Suppl., S1 (1989).
18. F. H. Allen, O. Kennard, D. G. Watson, et al., J. Chem. Soc., Perkin Trans. II, Suppl. S1 (1987).
19. A. W. Addison and T. N. Rao, J. Chem. Soc., Dalton Trans., 1349 (1984).
20. B. Chiari, W. E. Hatfild, O. Piovesana, et al., Inorg. Chem. **22**, 1468 (1983).
21. V. F. Shul'gin, O. V. Konnik, A. S. Bogomyakov, et al., Russ. J. Inorg. Chem. **57**, 615 (2012).
22. A. Yatani, M. Fujii, Y. Nakao, et al., Inorg. Chim. Acta **316**, 127 (2001).
23. R.-J. Tao, C.-Z. Mei, S.-Q. Zang, et al., Inorg. Chim. Acta **357**, 1985 (2004).
24. S. Thakurta, C. Rizzoli, R. J. Butcher, et al., Inorg. Chim. Acta **363**, 1395 (2010).

Translated by Z. Svitanko